

Supporting Information

A zirconium squarate metal-organic framework with modulator-dependent molecular sieving properties

Bart Bueken¹, Helge Reinsch¹, Nele Reimer², Ivo Stassen¹, Frederik Vermoortele,¹ Rob Ameloot,¹ Norbert Stock², Christine E.A. Kirschhock¹, Dirk De Vos^{1,*}

¹ Centre for Surface Chemistry and Catalysis, Katholieke Universiteit Leuven, Kasteelpark Arenberg 23 post box 2461, 3001 Leuven, Belgium

² Institut für Anorganische Chemie, Christian-Albrechts-Universität, Max-Eyth Straße 2, D 24118 Kiel, Germany

* Corresponding author. Tel.: +32 (0)16 32 16 39; Fax +32 (0)16 32 19 98; e-mail: dirk.devos@biw.kuleuven.be

Experimental section

Synthesis

All chemicals used to synthesize ZrSQU and HfSQU were commercially obtained from ABCR and Sigma-Aldrich and used without further purification. A typical synthesis of ZrSQU is performed in an 11 mL borosilicate glass reactor wherein 0.24 mmol (56 mg) $ZrCl_4$ is dissolved in a mixture of 64 mmol (5 mL) of *N,N*-dimethylformamide (DMF) and 70 mmol (4 mL) of acetic acid (AA). To this solution 0.72 mmol (82 mg) of SQA is added together with 12 mmol of HCl (1 mL HCl 37%). The molar ratio $ZrCl_4/SQA/HCl/H_2O/DMF/AA$ equals 1/3/50/174/267/292. This mixture is reacted at 383 K for 2-3 h, after which a white precipitate has formed (92 % yield based on Zr). The as-synthesized material is separated by centrifugation and washed several times with DMF and acetone followed by a drying step in air at 333 K for 24 h. Replacing $ZrCl_4$ with $HfCl_4$ enables the formation of the isostructural hafnium squarate. The use of a monocarboxylic modulator as well as HCl is required to obtain powder of sufficient crystallinity. ZrSQU can also be synthesized using formic acid (FA). In this case the optimal molar ratio $ZrCl_4/SQA/HCl/H_2O/DMF/FA$ is found to be 1/3/25/87/373/276. The synthesis and washing procedures are in each case identical as in the previously described method. In absence of modulator no product was formed. Similarly, in absence of DMF no crystallization occurred due to the low solubility of squaric acid in the resulting synthesis solution.

For reference, UiO-66 was prepared according to modified literature procedures^{1,2}. Zirconium fumarate was prepared according to the procedure published by Wißmann *et al.*³ employing 50 equivalents of acetic acid as modulator. Both materials were activated for gas sorption experiments by solvent exchange with DMF and methanol, followed by in air at 473 K for 24 h.

Materials characterization

Scanning electron microscopy (SEM) images and energy-dispersive X-ray spectroscopy (EDX) data were recorded on a Philips XL30 FEG microscope after sputtering with carbon. Thermogravimetric analyses were performed on a TA instruments TGA Q500. Samples were heated at a rate of 1 K min^{-1} to 673 K followed by 10 K min^{-1} to 1073 K under O_2 . Fourier transform infrared (FTIR) spectra were recorded on a NICOLET 6700 spectrometer (Thermo-Fischer) within the 500 cm^{-1} – 4000 cm^{-1} range (256 scans; 2 cm^{-1} resolution). Samples were analyzed as a self-supporting wafer of pure MOF or as a pellet of 5 wt% MOF in KBr. 1H liquid phase NMR spectra were obtained from activated ZrSQU samples (see section 'sorption experiments') dissolved in dimethylsulfoxide- d_6 (DMSO- d_6) according to the procedure proposed by Roy *et al.*⁴. Data was recorded on a Bruker AMX-300 spectrometer at 300 MHz for 1H (16 scans).

Samples were calibrated using a known amount of toluene to quantify the amount of modulator.

Sorption experiments

All sorption measurements were performed on a BELSORP-MAX instrument (BEL Japan Inc.). All ZrSQU samples were outgassed at 373 K under vacuum (10^{-4} bar) for 4 h. N₂ physisorption experiments were performed at 77 K within a p/p^0 range of $5 \cdot 10^{-5}$ – 0.994 (adsorption) and 0.994 – $8.5 \cdot 10^{-2}$ (desorption). Surface areas were calculated using the multi-point BET method applied to the isotherm's adsorption branch⁵. Hydrogen (H₂) adsorption experiments were conducted at 77 K between $8 \cdot 10^{-3}$ bar and 1.0037 bar H₂ pressure.

Synthesis & Optimization

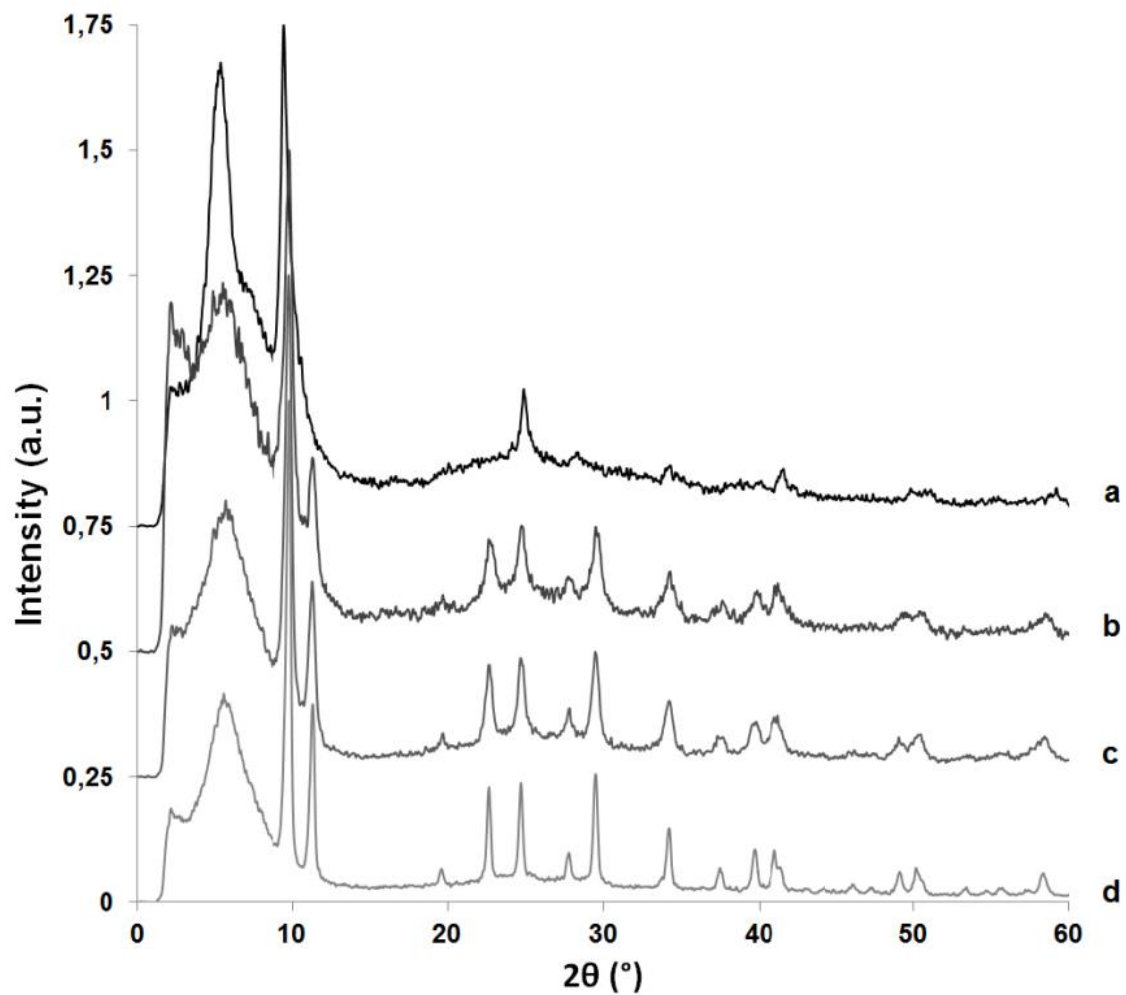


Figure S1: Powder diffractograms of materials obtained during synthesis optimization. Molar ratio versus Zr: HCl/AA 5/30 (a); HCl/AA 25/60 (b); HCl/AA 50/140 (c); HCl/AA 100/280 (d)

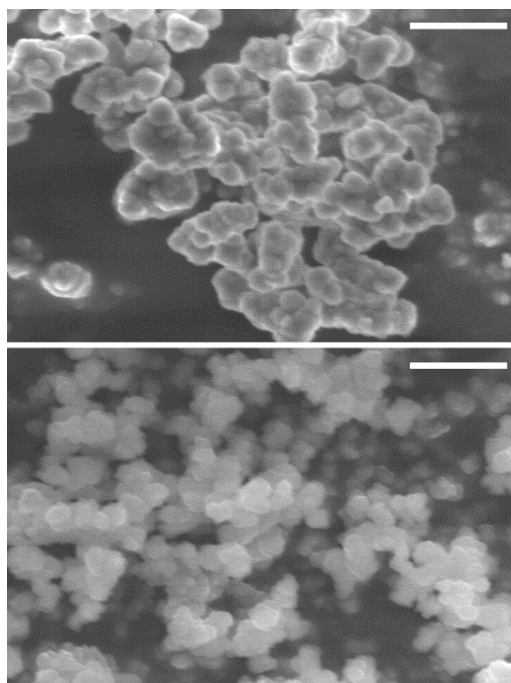
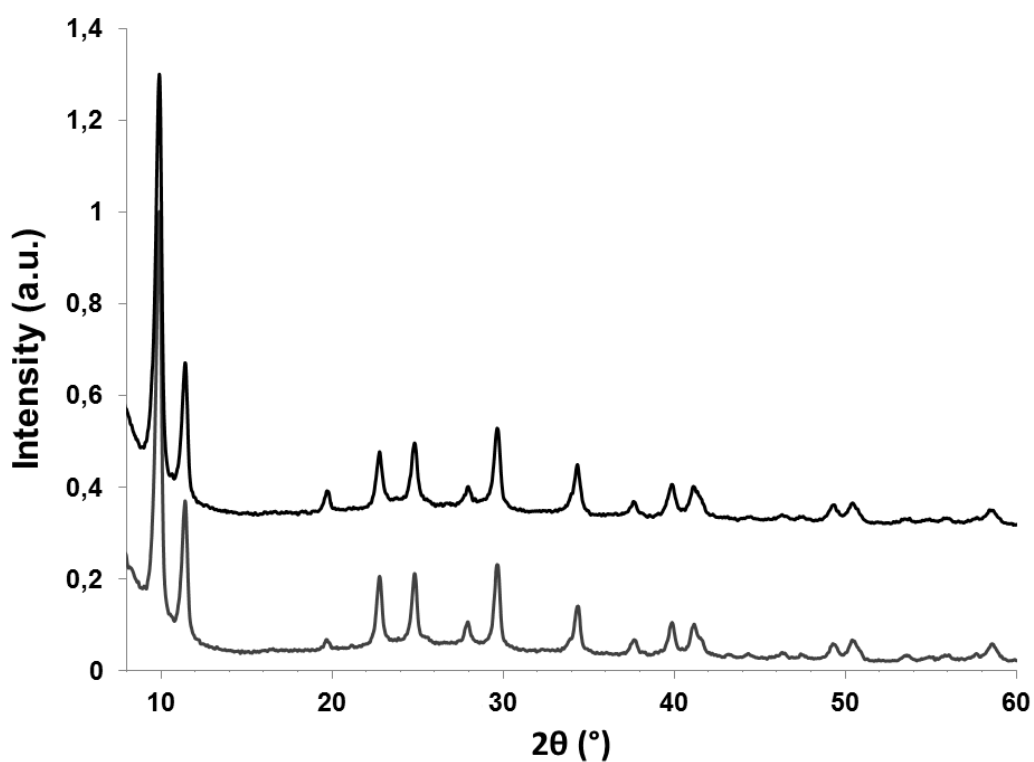


Figure S2: Top: Powder diffractograms of ZrSQU synthesized with formic acid (top) and acetic acid (bottom). Bottom: SEM images of ZrSQU synthesized in the presence of formic acid (top) and acetic acid (bottom), illustrating the small, highly aggregated crystallites. Scale bar: 2 μm .

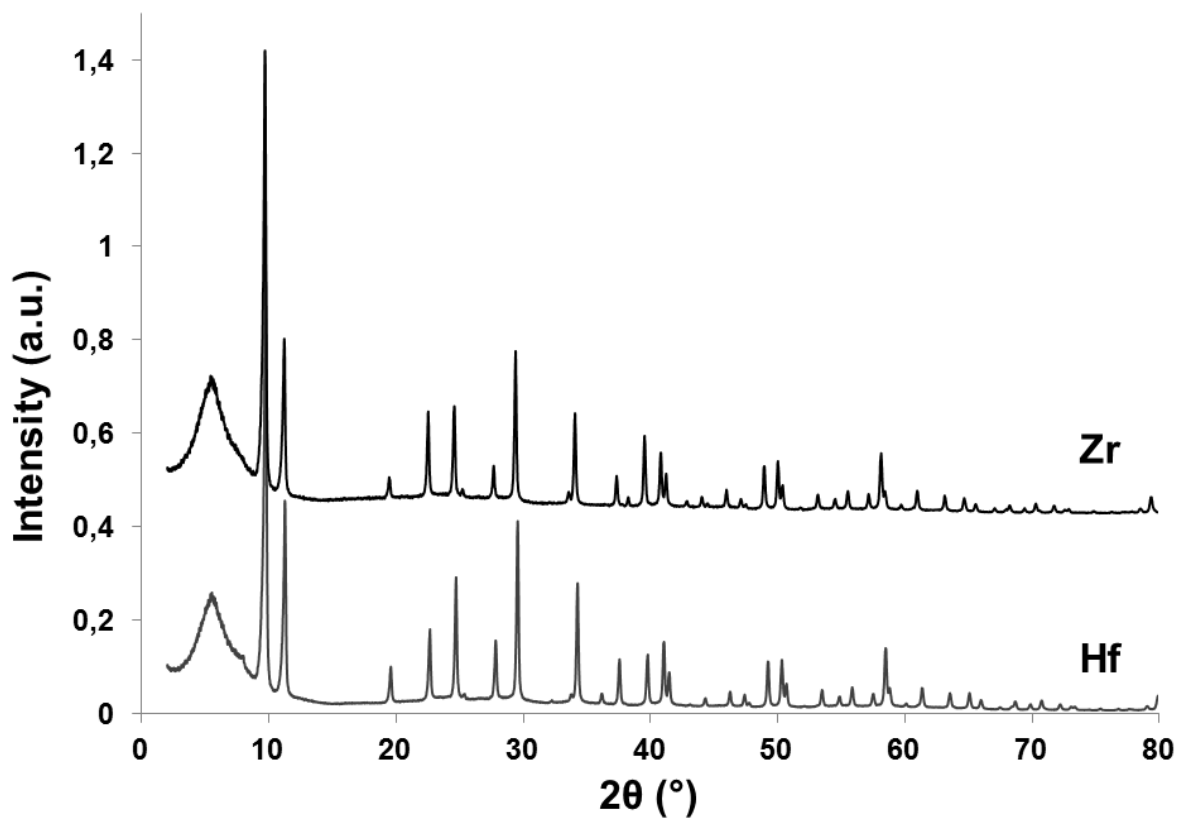


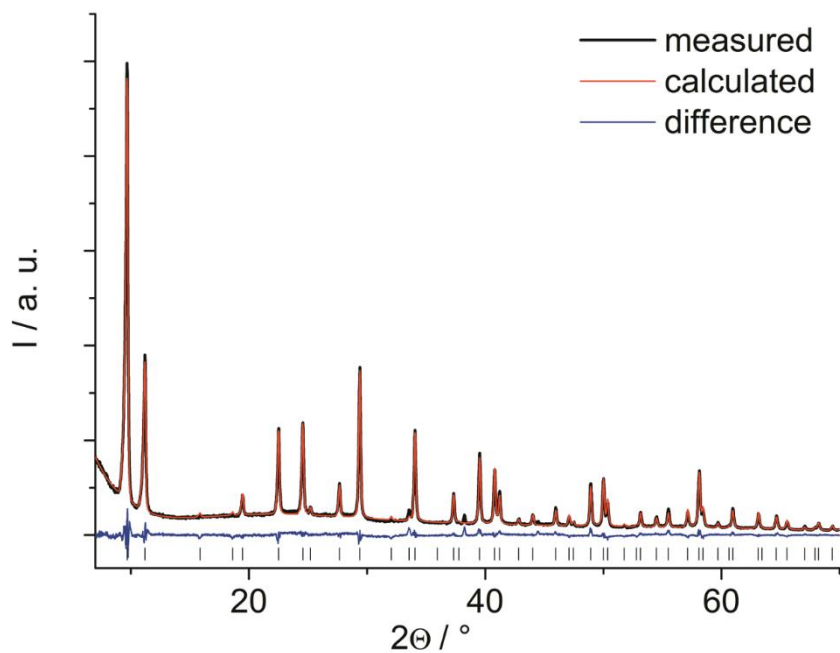
Figure S3: High resolution powder diffractograms of ZrSQU_A (top) and HfSQU_A (bottom).

Crystal structure determination

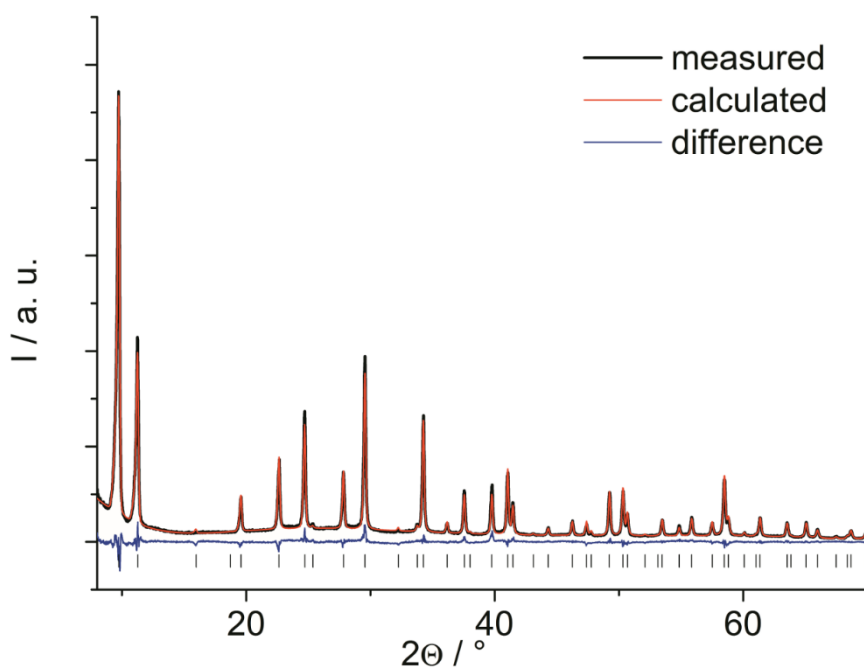
High-resolution powder x-ray diffraction (PXRD) data were recorded on a STOE Stadi P in Bragg-Brentano mode (2θ - θ geometry; monochromated $\text{CuK}\alpha$ -radiation, $\lambda = 1.54060 \text{ \AA}$) equipped with a linear PSD detector system in transmission geometry. High-throughput PXRD data were obtained on a STOE COMBI P diffractometer (monochromated $\text{CuK}\alpha$ -radiation, $\lambda = 1.54060 \text{ \AA}$) equipped with an IP-PSD detector in transmission geometry. All cell indexing and Rietveld refinements were carried out using TOPAS, version 4.1⁶. As a starting point for the Rietveld-refinement, a structural model was set up using Materials Studio, version 4.3⁷. Pore accessible volume and pore sizes were analyzed with the PLATON⁸ and Zeo++⁹ software using a 1.2 \AA probe.

High resolution PXRD diffractograms for both ZrSQU and HfSQU synthesized with acetic acid as modulator were successfully indexed with a cubic cell (ZrSQU: $a = 15.784(3) \text{ \AA}$; HfSQU: $a = 15.690(3) \text{ \AA}$) and extinction conditions consistent with the space group $Fm-3m$ (n° 225). The broad reflection centered around $5.5^\circ 2\theta$ was omitted for structure solution. As the $Fm-3m$ space group is identical to that of the zirconium terephthalate UiO-66¹, its crystal structure was taken as a basis for structure solution. An initial structural model was set up using the Materials Studio software by substituting the C-C₆H₄-C linker fragments in UiO-66(Hf) by the cyclic C₄ fragment in SQU, effectively conserving the positions of the carboxylate oxygen atoms. This model was subsequently relaxed by force field geometry optimization (Forcite module) while imposing the cell parameters obtained by powder pattern indexing. The resulting model was Rietveld refined using the TOPAS software. Any residual electron density in the pores of the framework, as found by Fourier synthesis, was modelled by oxygen atoms partially occupying these positions. The refined structure of HfSQU was used as a starting model in the Rietveld refinement of ZrSQU after substitution of Hf for Zr.

The broad reflection centered around 5.5 \AA , which is forbidden for $Fm-3m$, is believed to be caused by the presence of a primitive superstructure of the ZrSQU lattice. This has been described previously for UiO-66 where additional forbidden reflections were fitted by a model with the same cell parameters in the primitive $Pm-3m$ space group^{10,11}



Final Rietveld plot of the refinement of ZrSQU_A. Observed intensities, calculated intensities and the difference curve are represented in black, red and blue respectively.



Final Rietveld plot of the refinement of HfSQU_A. Observed intensities, calculated intensities and the difference curve are represented in black, red and blue respectively.

Table S1: Final Rietveld refinement parameters for ZrSQU_A and HfSQU_A.

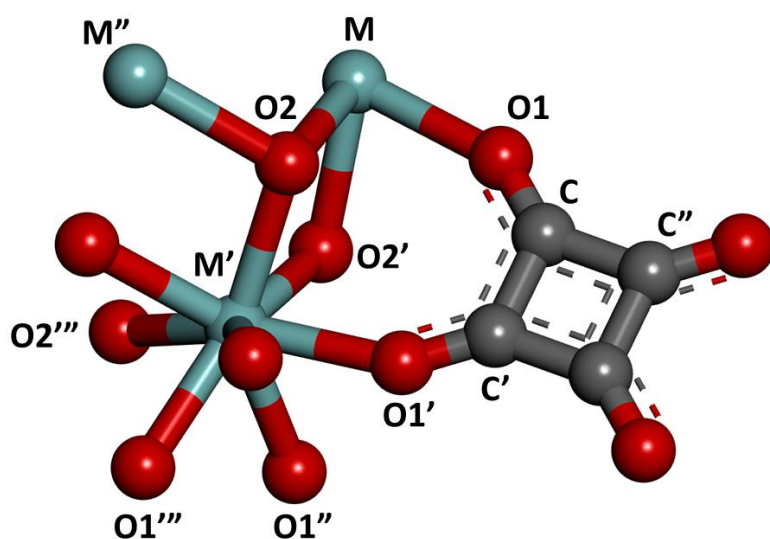
compound	ZrSQU	HfSQU
crystal system	cubic	cubic
space group	<i>Fm-3m</i> (n° 225)	<i>Fm-3m</i> (n° 225)
$a=b=c$ (Å)	15.78376(17)	15.69022(16)
V (Å ³)	3932.18(7)	3862.67(7)
R_{wp} (%)	6.4	7.1
R_{Exp} (%)	4.8	5.6
R_{Bragg} (%)	2.3	3.7
GoF	2.9	2.9

Table S2: Atomic coordinates and temperature factors for ZrSQU_A

Atom	a	b	c	occupancy	B_{iso} (Å ²)
Zr	0.15815(11)	0.000000	0.000000	1.0000	0.232
O1	0.2415(4)	0.000000	0.1092(3)	1.0000	3.690
O2	0.0844(4)	0.0844(4)	0.0844(4)	1.0000	3.690
C	0.2499(4)	0.000000	0.1849(3)	0.7510	3.690
Ox1	0.2989(7)	0.1662(14)	0.2989(7)	0.3270	7.970
Ox2	0.5520(13)	0.5520(13)	0.415(2)	0.1930	7.970

Table S3: Atomic coordinates and temperature factors for HfSQU_A

Atom	a	b	c	occupancy	B_{iso} (Å ²)
Hf	0.158480(89)	0.000000	0.000000	1.0000	1.149(74)
O1	0.24805(58)	0.000000	0.10573(21)	1.0000	4.51(23)
O2	-0.08124(48)	0.08124(48)	0.08124(48)	1.0000	4.51(23)
C	0.24990(59)	0.18244(42)	0.721(10)	0.721(10)	4.51(23)
Ox1	0.30096(79)	0.1591(17)	0.2989(7)	0.30096(79)	0.1(11)



Atom labels used in Tables S4 and S5.

Table S4: Bond lengths (in Å) and interatomic distances for ZrSQU and HfSQU calculated using PLATON.

	M = Zr	M = Hf
M – O1	2.168(6)	2.174(7)
M – O2	2.215(6)	2.172(8)
O1 – C	1.202(9)	1.204(9)
C – C'	1.451(9)	1.498(12)
C – C''	1.455	1.502
M – M'	3.530	3.517

Table S5: Bond angles (in °) for ZrSQU and HfSQU calculated using PLATON.

	M = Zr	M = Hf
M – O2 – M'	105.7(3)	108.1(3)
O2 – M – O1	80.8(2)	85.0(3)
O2 – M – O2'	74.0(2)	71.8(3)
O2 – M' – O2'''	116.6(2)	112.1(3)
O1' – M' – O2'''	142.85(12)	144.0(2)
O1' – M' – O1''	68.40(13)	65.28(16)
O1' – M' – O1'''	105.3(2)	99.4(3)
M – O1 – C	149.0(5)	141.1(8)
O1 – C – C'	128.7(6)	133.7(9)
O1 – C – C''	141.30	136.33
C' – C – C''	90.00	90.00

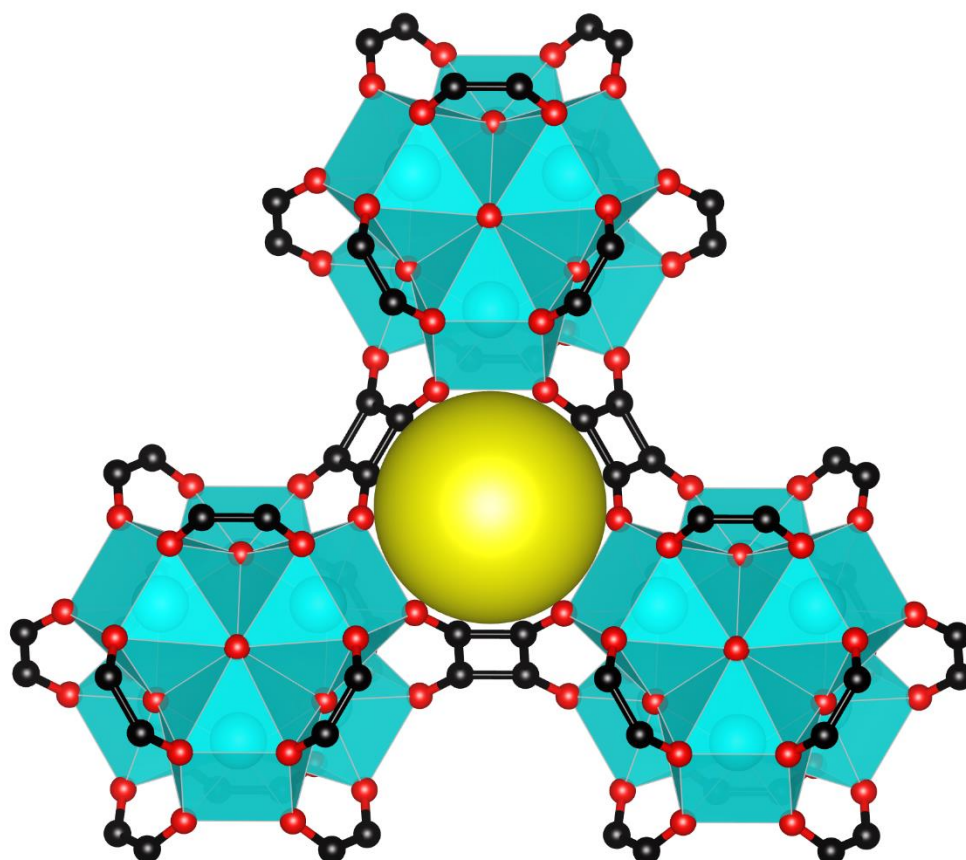


Figure S4: triangular window of ZrSQU. The diameter of the largest sphere that can pass through this window (taking into account the Van der Waals surface) is 2.4 Å

Characterization: FTIR

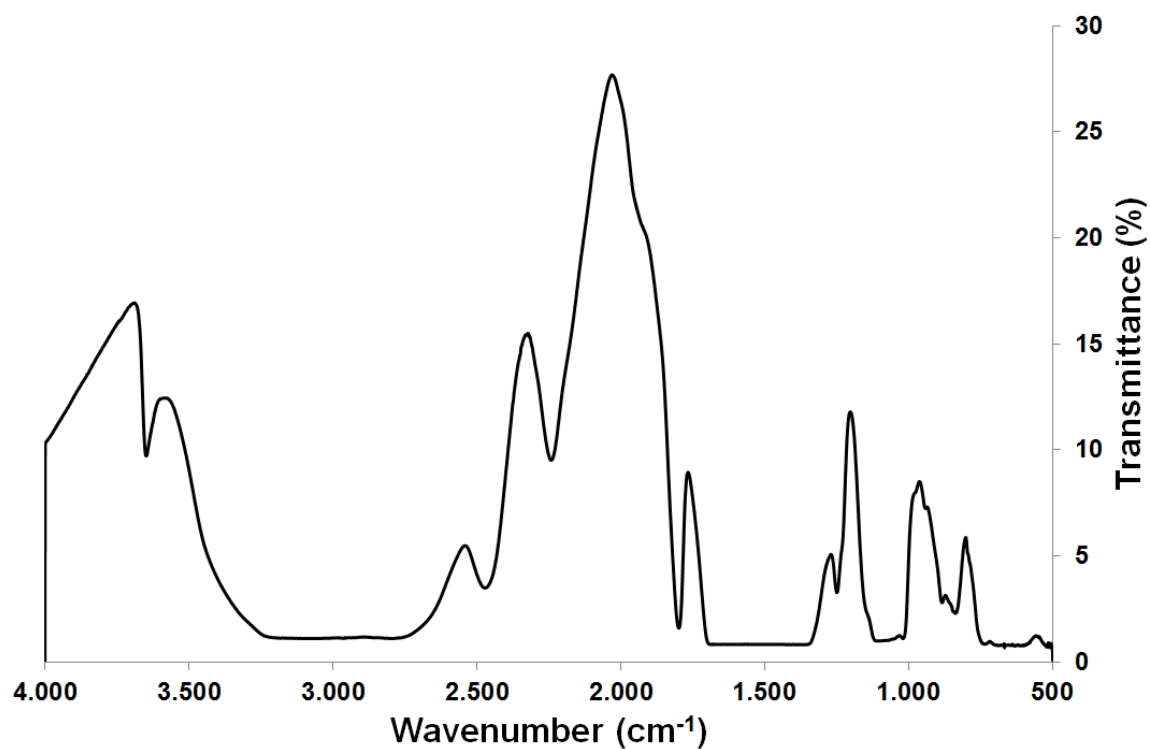
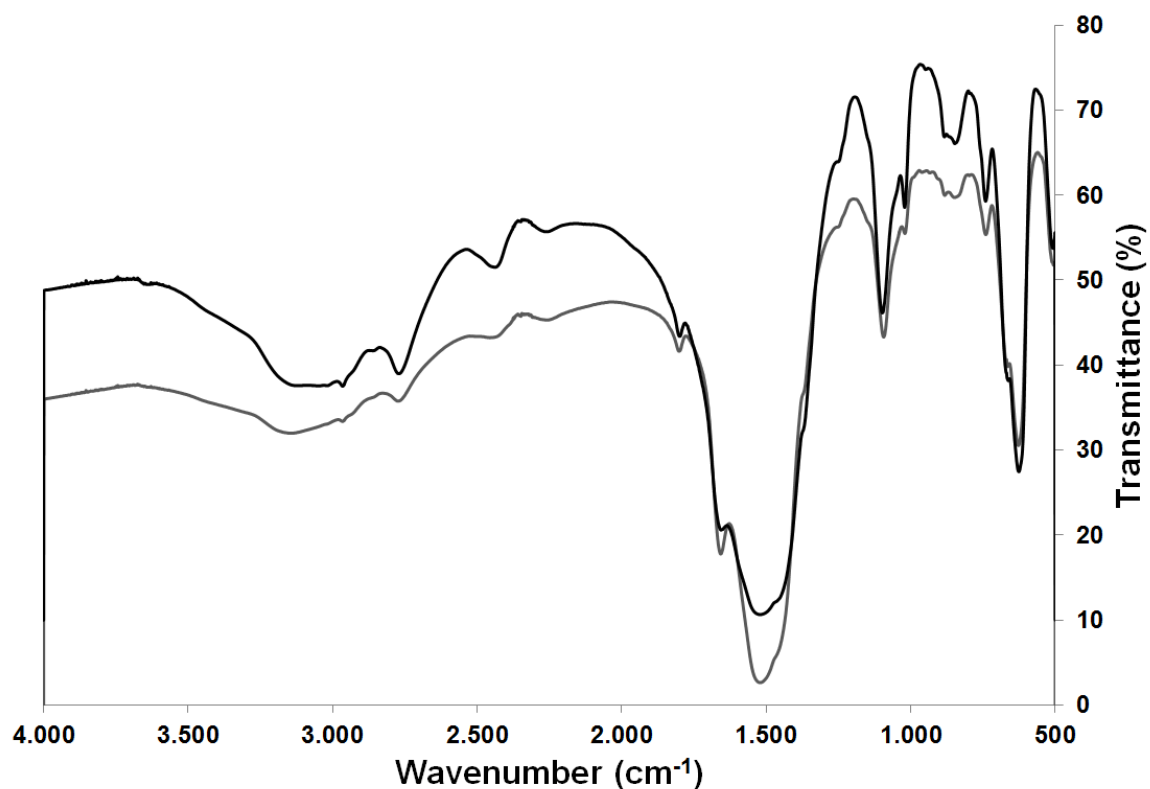


Figure S5: Top: FTIR spectra of ZrSQU_A in KBr (As synthesized: black; Activated: grey). Bottom: FTIR spectrum of pure as synthesized ZrSQU_A

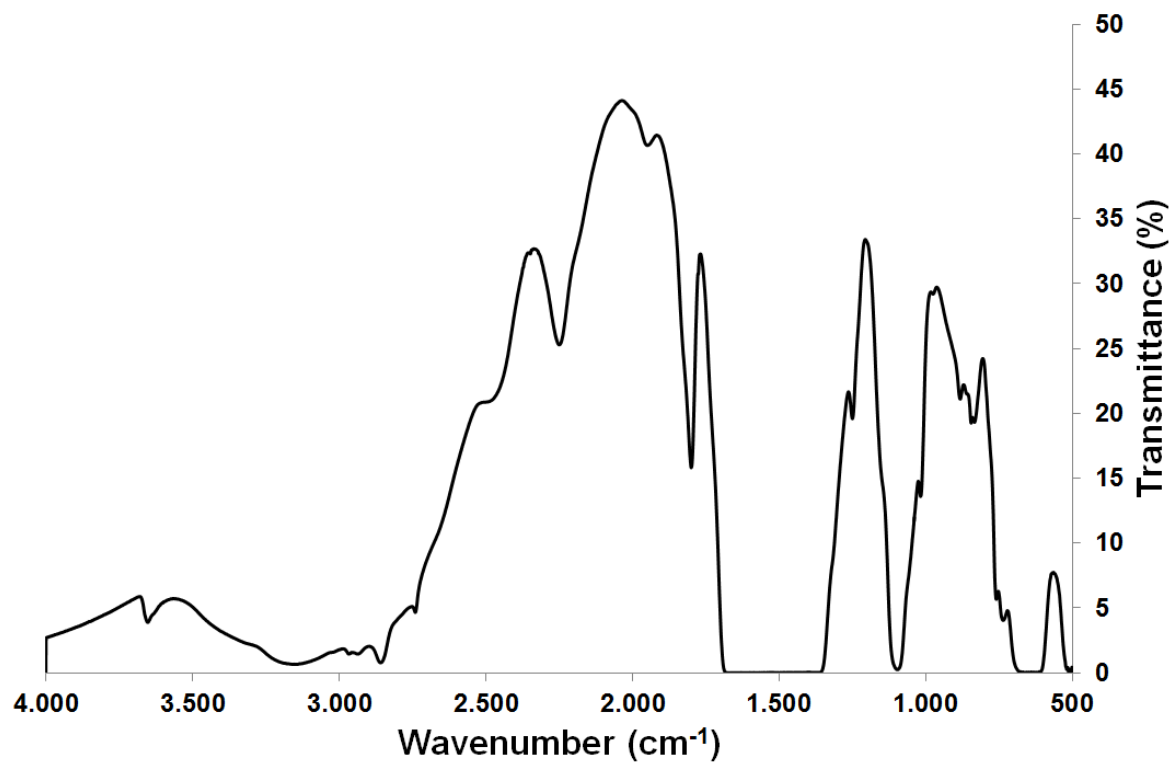
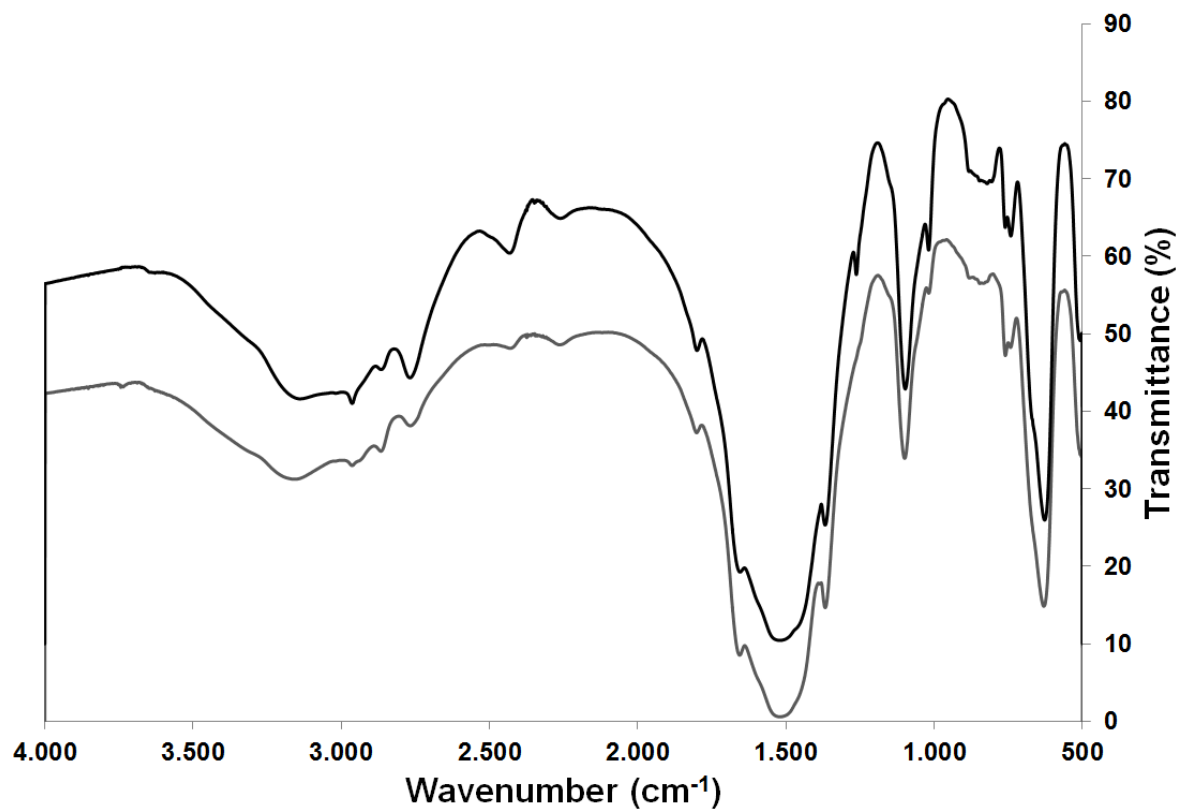


Figure S6: Top: FTIR spectra of ZrSQU_F in KBr (As synthesized: black; Activated: grey). Bottom: FTIR spectrum of pure as synthesized ZrSQU_F

Characterization: TG Analysis

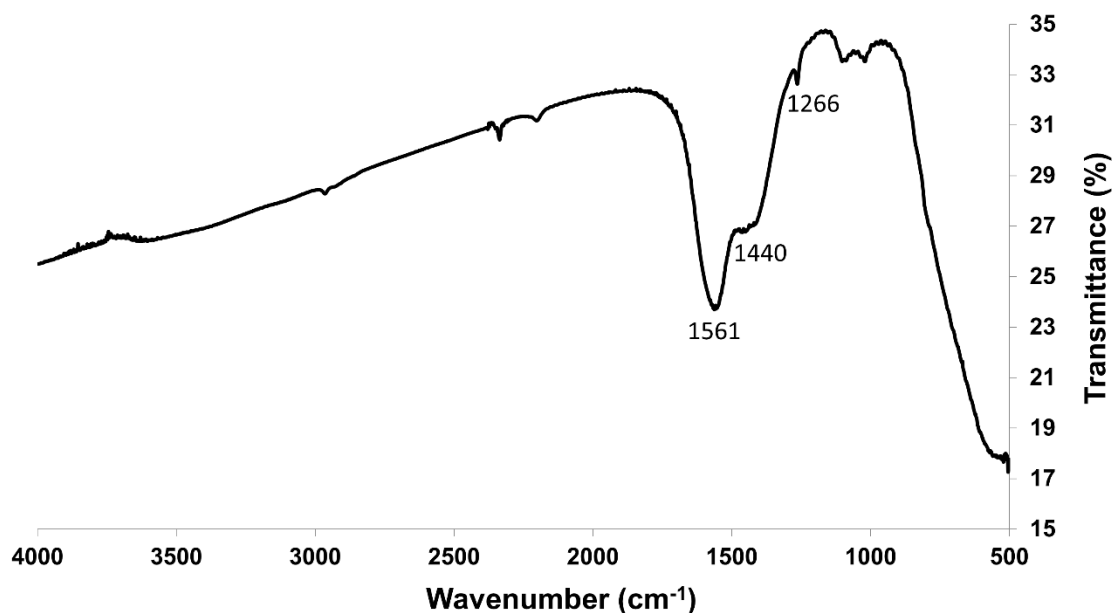


Figure S7: FTIR spectrum of ZrSQU_A calcined at 723 K in air. The bands centered at 1561 cm⁻¹, 1440 cm⁻¹ and 1266 cm⁻¹ are indicative for carbonate species.

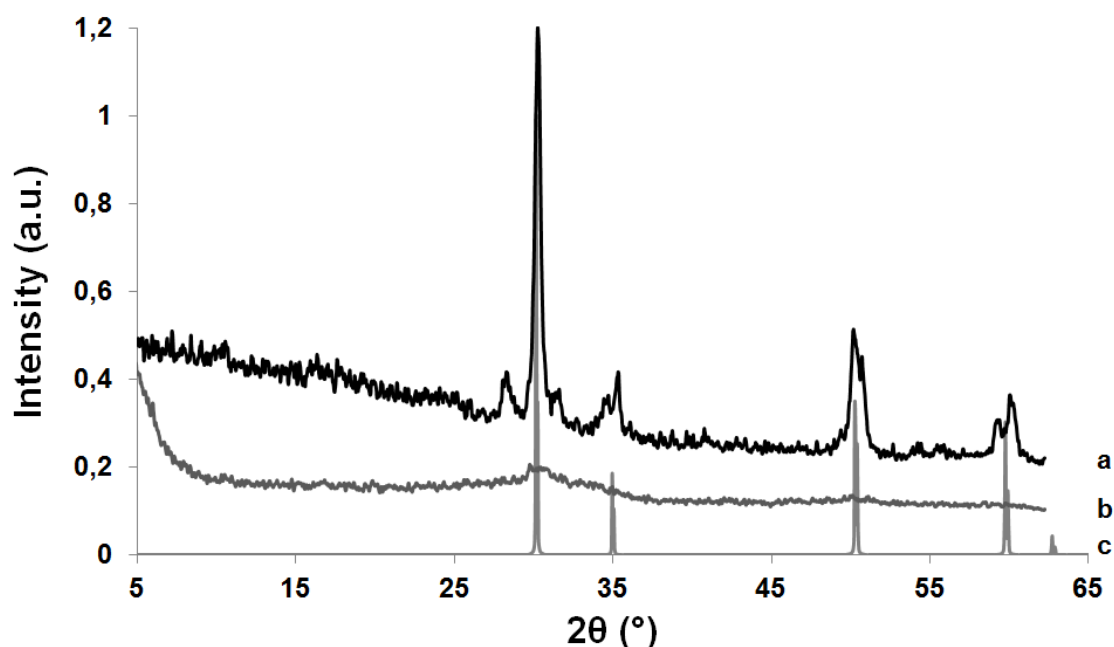


Figure S8: PXRD patterns of ZrSQU_A calcined to 800 °C (a) and ZrSQU_A calcined to 450 °C (b). The former corresponds to tetragonal zirconia as evidenced by the reference diffraction pattern (c).

Influence of activation on crystallinity

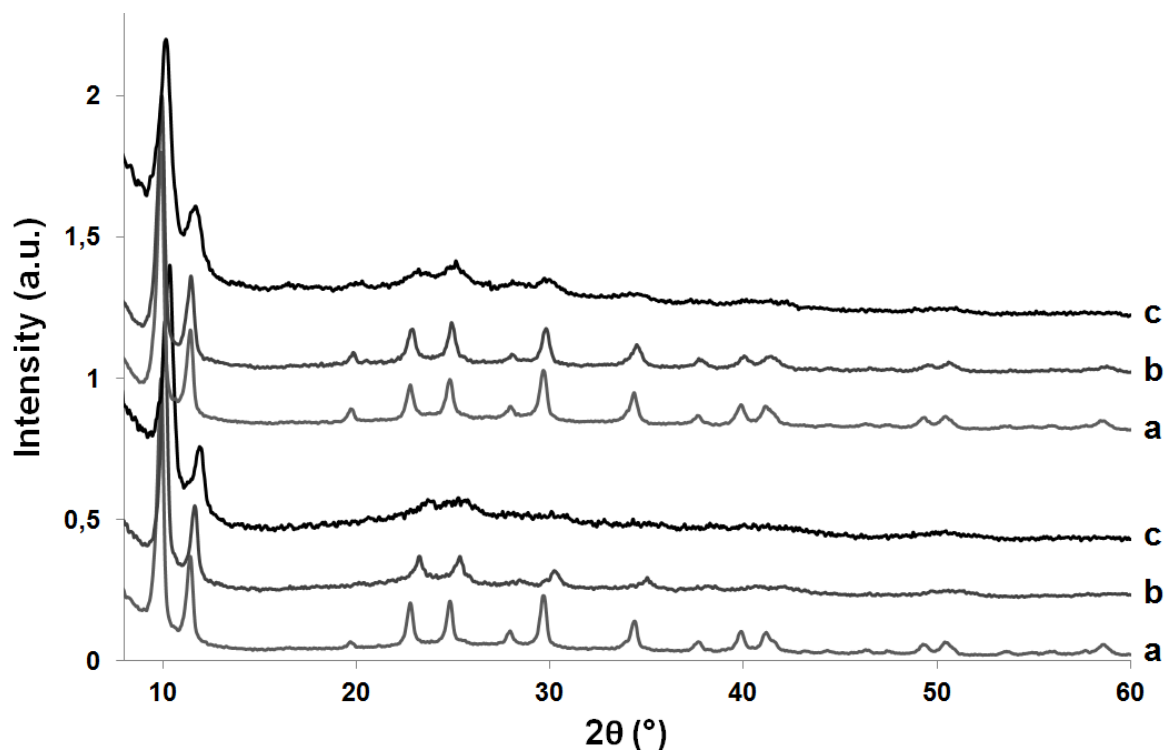


Figure S9: PXRD patterns of ZrSQU_F (top) and ZrSQU_A (bottom). The as synthesized material (a) can be washed with DMF without influence on the structure (b). Thermal treatment (373 K) under vacuum results in loss of long range order (c).

Water stability of ZrSQU

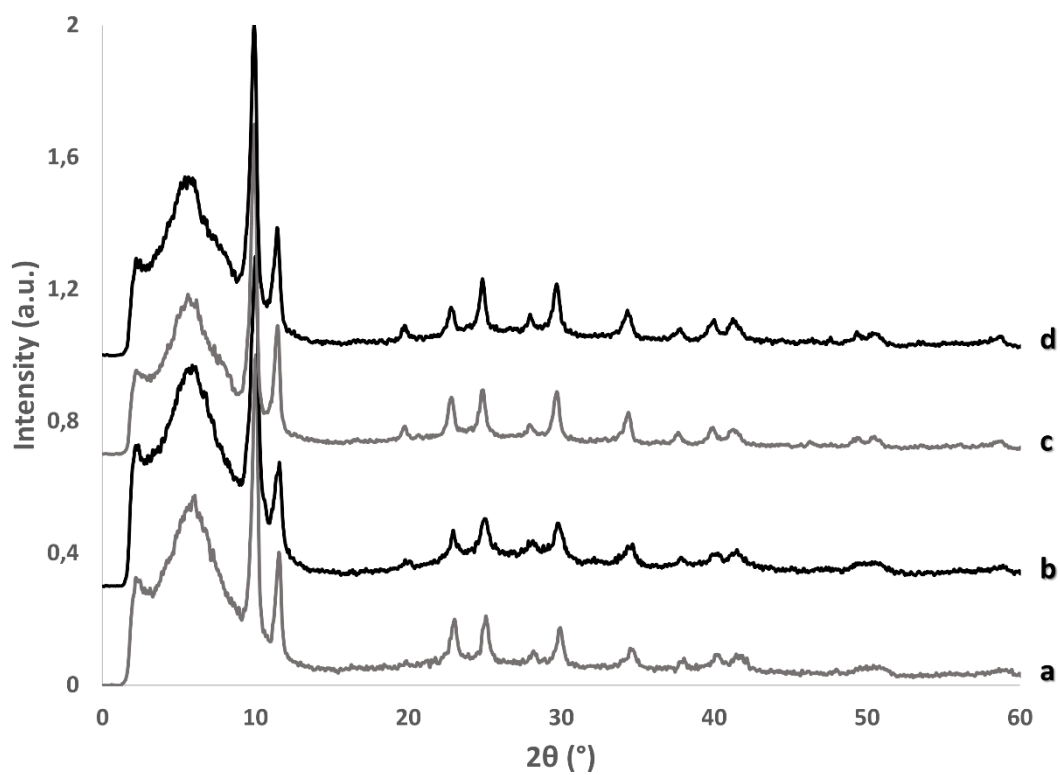


Figure S10: PXRD patterns of ZrSQU_A (a, b) and ZrSQU_F (c, d). The DMF-washed materials (a, c) retain their crystallinity after soaking in water for 72 h (b, d).

Characterization: EDX spectra

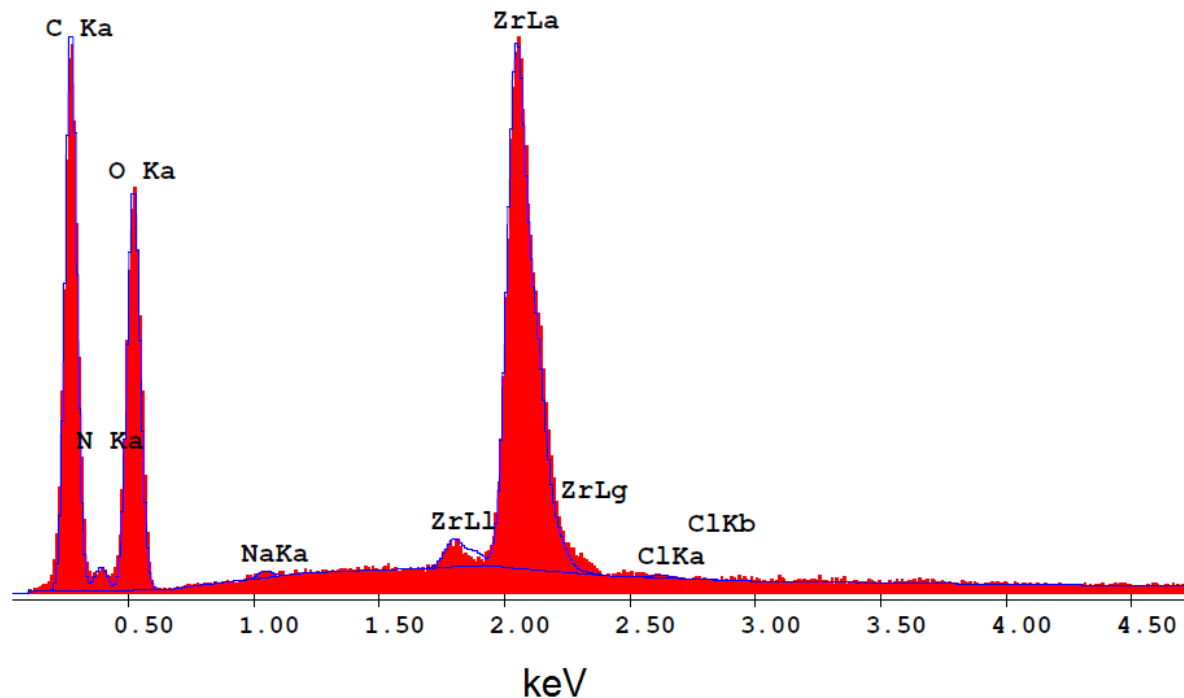
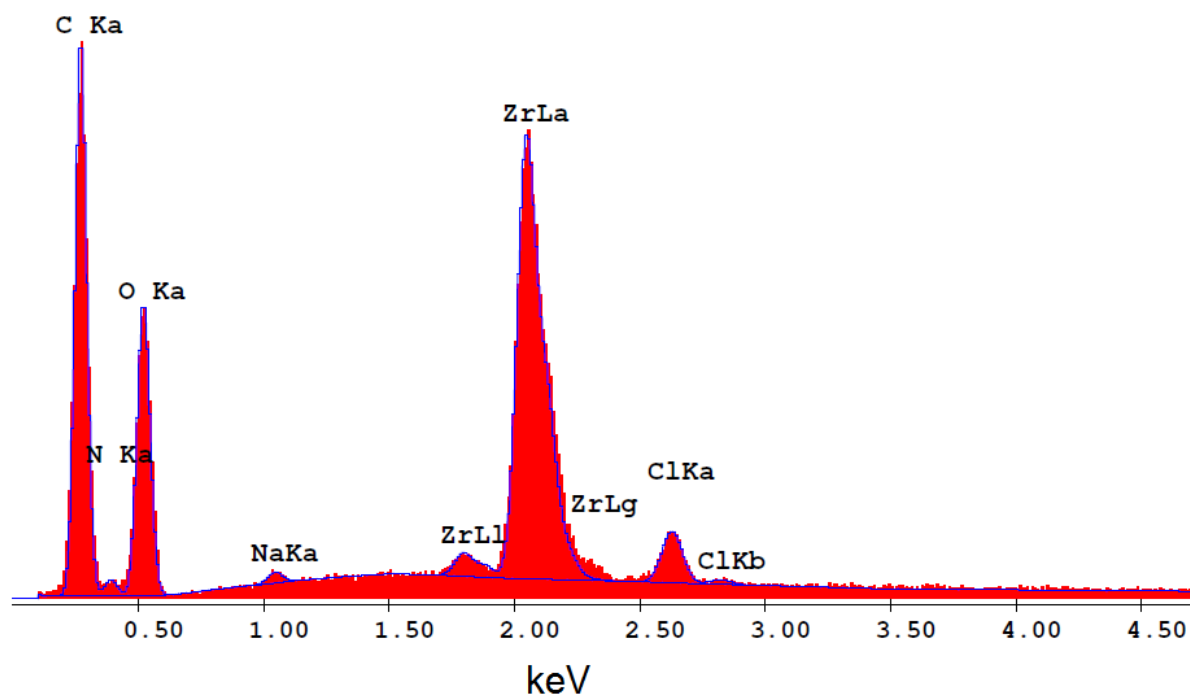


Figure S11a: EDX spectra of ZrSQUA as synthesized (top) and after washing (bottom).

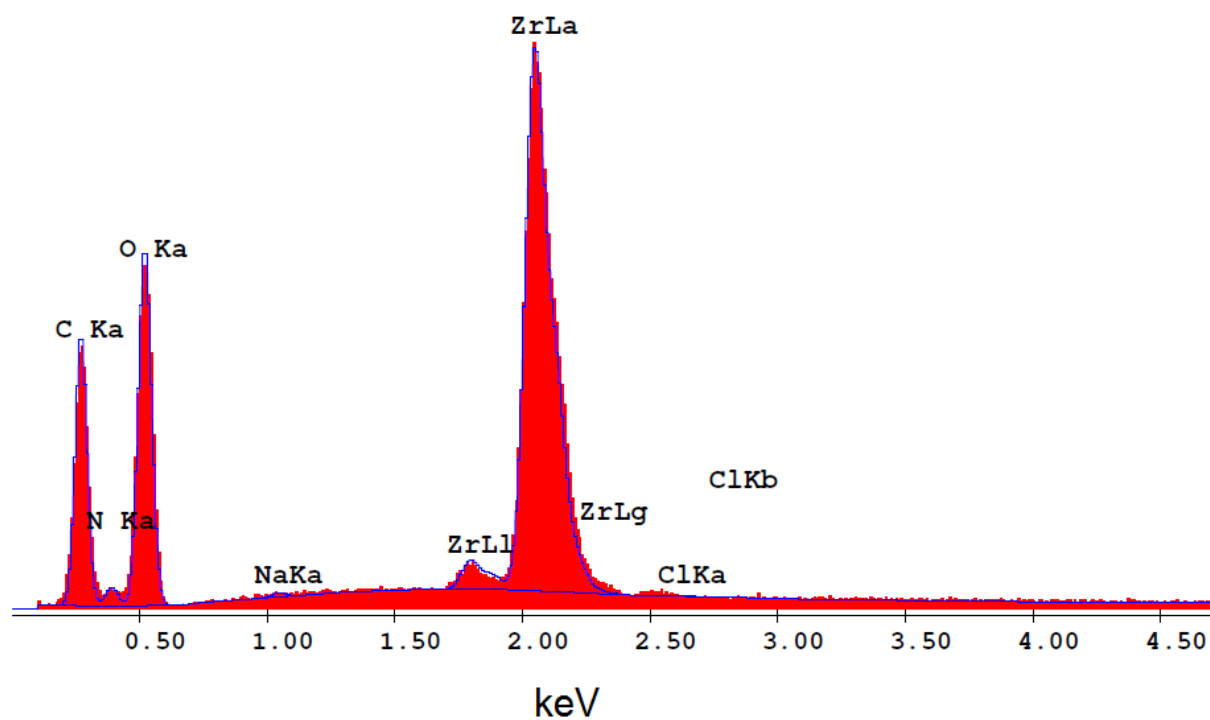
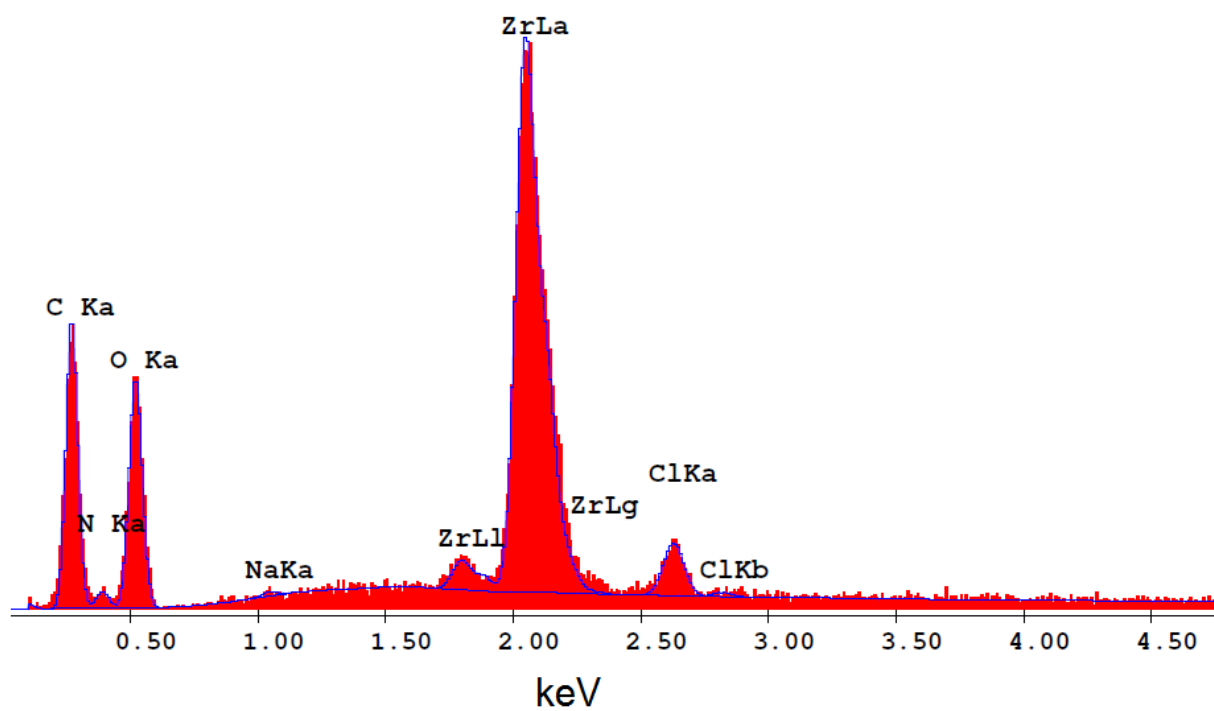


Figure S11b: EDX spectra of ZrSQU_F as synthesized (top) and after washing (bottom).

Comparison of sorption properties to other Zr-MOFs

The tunable microporosity of ZrSQU can be exploited in gas purifications. In order to appreciate ZrSQU's potential, the amount of adsorbed gas molecules per unit cell (equivalent to two octahedral and four tetrahedral cages) was calculated based on the experimental results. For comparison, the same values were determined for the isorecticular UiO-66 (linker length 7.01 Å) and Zr-fumarate (linker length 5.11 Å) MOFs. As can be seen from Table S6, both UiO-66 and Zr-fumarate have a much larger uptake capacity for both H₂ and N₂ due to their substantially larger accessible volume. However, neither of these Zr-MOFs can discriminate between H₂ and N₂ based on size. The same can be said for ZrSQU_F, which shows similar uptake for H₂ and N₂. ZrSQU_A on the other hand clearly features a preference for H₂ adsorption.

Table S6: Single compound adsorption of gas molecules per unit cell at 77 K. For H₂ the maximum uptake was used, for N₂ the micropore uptake was used. Prior to measurements UiO-66 and Zr-fumarate were activated at 473 K under vacuum (10⁻⁴ bar) for 12 h

	ZrSQU _{AA}	ZrSQU _{FA}	Zr-fumarate	UiO-66
V _{sa} (Å ³)	1283.5 ^a (32.6%)		2347.9 (44.4%)	5282.0 (57.4%)
Window diameter (Å)	2.4		not available	6 ¹
Linker length (Å)	3.61		5.11	7.01
N ₂	1	10	45	80
H ₂	9	12	35	49
Ratio H ₂ /N ₂	9	1.2	0.8	0.6

V_{sa}: maximal solvent accessible volume per unit cell as calculated by PLATON⁸, probe radius 1.2 Å; ^a: based on perfect Zr₆O₄(OH)₄(C₄O₄)₆ crystal structure.

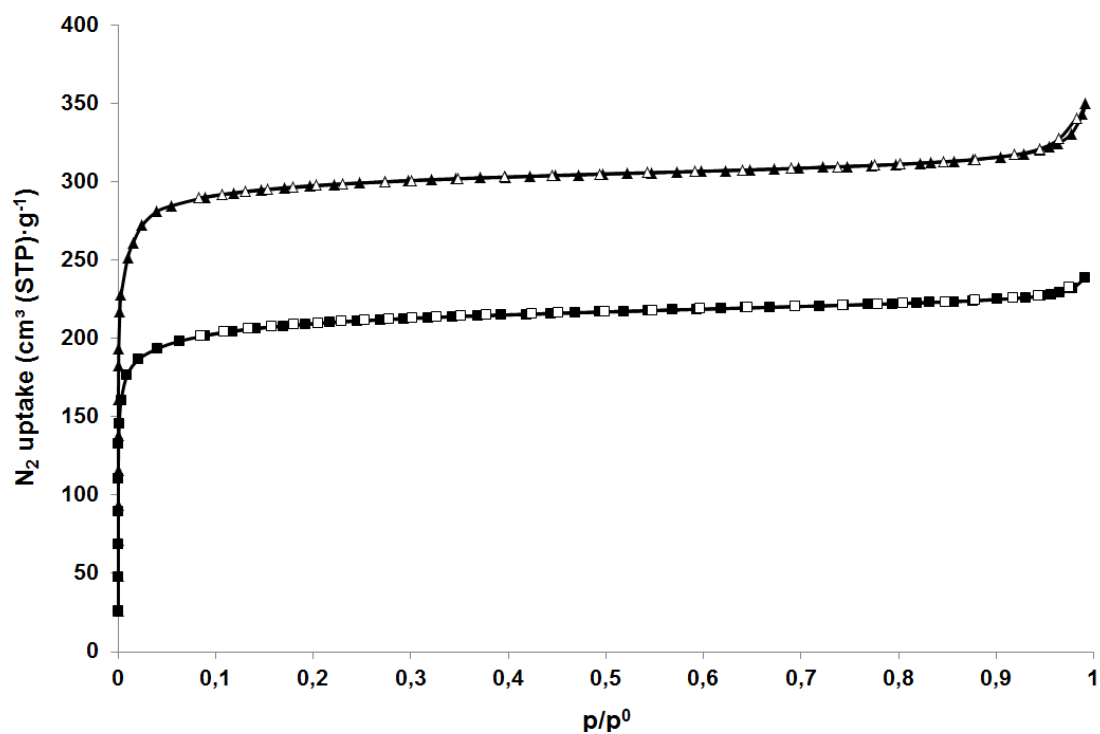


Figure S12: N₂ physisorption isotherms for UiO-66 (triangles) and Zr-fumarate (squares) at 77K. Full symbols: adsorption; Open symbols: desorption.

Table S7: Specific surface area, and N₂ sorption properties for ZrSQU

	S_{BET} (m ² ·g ⁻¹)	V_p (cm ³ ·g ⁻¹)	V_{max} (cm ³ (STP)·g ⁻¹)
Zr-fumarate	809	0.34	186
UiO-66	1177	0.47	270

S_{BET} : BET surface area calculated via the Rouquerol method¹²; V_p : total pore volume at $p/p^0 = 0.500$; V_{max} = maximal N₂ uptake in micropores

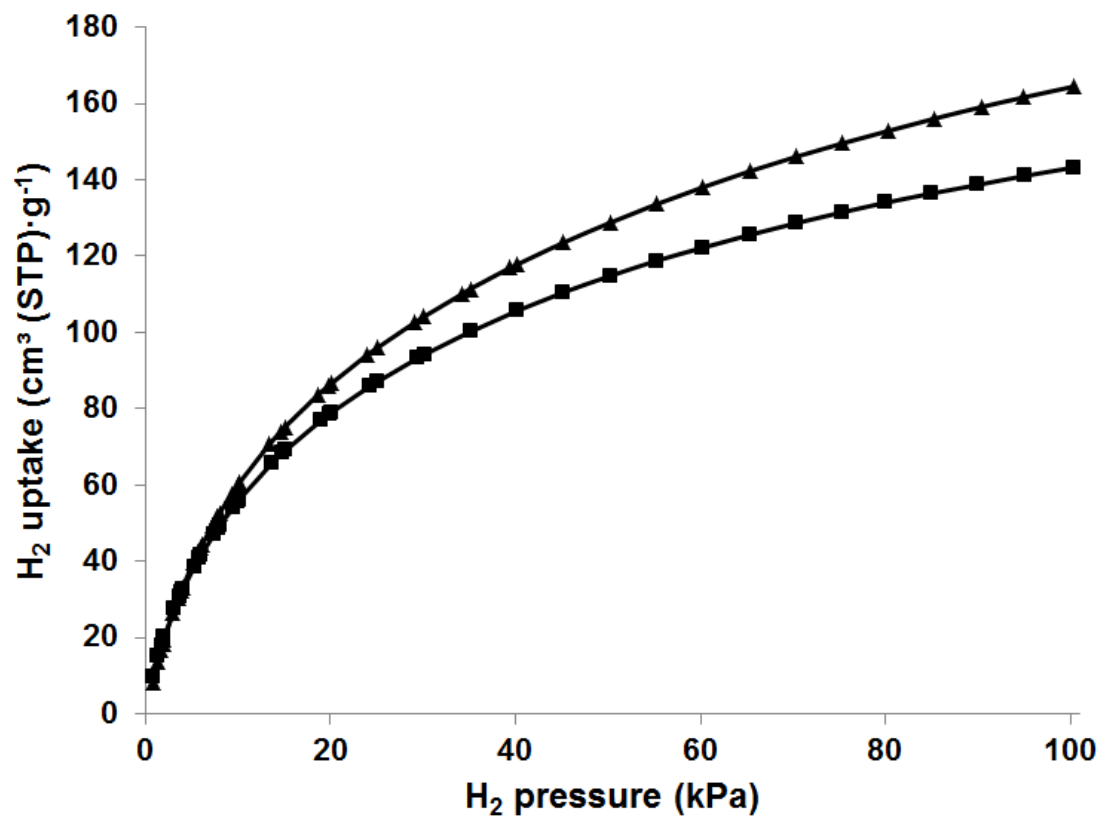


Figure S13: Hydrogen adsorption isotherms for UiO-66 (triangles) and Zr-fumarate (squares) at 77 K.

Literature

1. J. H. Cavka, S. Jakobsen, U. Olsbye, N. Guillou, C. Lamberti, S. Bordiga, and K. P. Lillerud, *J. Am. Chem. Soc.*, 2008, **130**, 13850–1.
2. M. J. Katz, Z. J. Brown, Y. J. Colón, P. W. Siu, K. A. Scheidt, R. Q. Snurr, J. T. Hupp, and O. K. Farha, *Chem. Commun.*, 2013.
3. G. Wißmann, A. Schaate, S. Lilienthal, I. Bremer, A. M. Schneider, and P. Behrens, *Microporous Mesoporous Mater.*, 2012, **152**, 64–70.
4. P. Roy, A. Schaate, P. Behrens, and A. Godt, *Chemistry*, 2012, **18**, 6979–85.
5. J. Rouquerol, F. Rouquerol, and K. S. W. Sing, *Absorption by Powders and Porous Solids*, 1998.
6. A. A. Coelho, 2007.
7. Accelrys Inc., 2008.
8. A. L. Spek, *Acta Crystallogr. D. Biol. Crystallogr.*, 2009, **65**, 148–55.
9. T. F. Willems, C. H. Rycroft, M. Kazi, J. C. Meza, and M. Haranczyk, *Microporous Mesoporous Mater.*, 2012, **149**, 134–141.
10. M. Kandiah, M. H. Nilsen, S. Usseglio, S. Jakobsen, U. Olsbye, M. Tilset, C. Larabi, E. A. Quadrelli, F. Bonino, and K. P. Lillerud, *Chem. Mater.*, 2010, **22**, 6632–6640.
11. S. Jakobsen, D. Gianolio, D. Wragg, M. H. Nilsen, H. Emerich, S. Bordiga, C. Lamberti, U. Olsbye, M. Tilset, and K. Lillerud, *Phys. Rev. B*, 2012, **86**.
12. J. Rouquerol, P. L. Llewellyn, and F. Rouquerol, *Stud. Surf. Sci. Catal.*, 2007, **166**, 49–56.